

Structural and compositional dependence of gadolinium-aluminum oxide for the application of charge-trap-type nonvolatile memory devices

Youngmin Park, Jong Kyung Park, Myeong Ho Song, Sung Kyu Lim, Jae Sub Oh, Moon Sig Joo, Kwon Hong , and Byung Jin Cho

Citation: [Applied Physics Letters](#) **96**, 052907 (2010); doi: 10.1063/1.3309693

View online: <http://dx.doi.org/10.1063/1.3309693>

View Table of Contents: <http://scitation.aip.org/content/aip/journal/apl/96/5?ver=pdfcov>

Published by the [AIP Publishing](#)

Articles you may be interested in

[Impact of composition and crystallization behavior of atomic layer deposited strontium titanate films on the resistive switching of Pt/STO/TiN devices](#)

[J. Appl. Phys.](#) **116**, 064503 (2014); 10.1063/1.4891831

[Performance improvement of metal-Al₂O₃-HfO₂-oxide-silicon memory devices with band-engineered Hf-aluminate/SiO₂ tunnel barriers](#)

[J. Vac. Sci. Technol. B](#) **31**, 041201 (2013); 10.1116/1.4807842

[Experimental evidence and modeling of two types of electron traps in Al₂O₃ for nonvolatile memory applications](#)

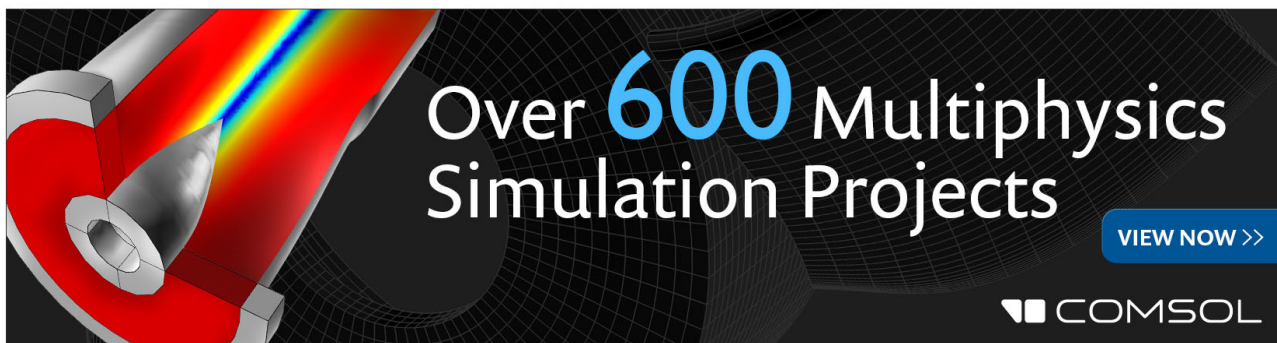
[J. Appl. Phys.](#) **113**, 074501 (2013); 10.1063/1.4792038

[Effects of rapid thermal annealing on structure and electrical properties of Gd-doped HfO₂ high k film](#)

[Appl. Phys. Lett.](#) **98**, 082906 (2011); 10.1063/1.3556652

[Low temperature crystallization of high permittivity Ta oxide using an Nb oxide thin film for metal/insulator/metal capacitors in dynamic random access memory applications](#)

[J. Vac. Sci. Technol. B](#) **23**, 80 (2005); 10.1116/1.1829060

The advertisement features a dark background with a grid pattern. On the left, there is a 3D cutaway view of a mechanical part with a red and yellow color gradient. The text 'Over 600 Multiphysics Simulation Projects' is prominently displayed in white and blue. A blue button with the text 'VIEW NOW >>' is located on the right. The COMSOL logo is in the bottom right corner.

Over 600 Multiphysics Simulation Projects

VIEW NOW >>

COMSOL

Structural and compositional dependence of gadolinium-aluminum oxide for the application of charge-trap-type nonvolatile memory devices

Youngmin Park,¹ Jong Kyung Park,¹ Myeong Ho Song,² Sung Kyu Lim,² Jae Sub Oh,² Moon Sig Joo,³ Kwon Hong,³ and Byung Jin Cho^{1,a)}

¹Department of Electrical Engineering, Korea Advanced Institute of Science and Technology, 373-1 Guseong-dong, Yuseong-gu, Daejeon 305-701, Republic of Korea

²National Nanofab Center, 373-1 Guseong-dong, Yuseong-gu, Daejeon 305-701, Republic of Korea

³Hynix Semiconductor Inc., San 136-1, Ami-ri, Bubal-eub, Icheon-si, Gyeonggi-do 467-701, Republic of Korea

(Received 11 December 2009; accepted 15 January 2010; published online 5 February 2010)

The structural and compositional dependence of gadolinium-aluminum oxide (GdAlO) for application to nonvolatile memory is investigated. An addition of Gd into AlO reduces the leakage current, which improves the erase window. The GdAlO film crystallizes into many different phases after annealing depending on the Gd percentage when the amount of Gd exceeds 49%. The crystallization of the GdAlO film causes a change in the band gap of the GdAlO film, resulting in a change of the retention properties. It is also found that crystallized GdAlO is more vulnerable to the generation of traps by electrical stress. The results indicate that careful optimization of the Gd percentage in GdAlO is necessary to utilize the benefit of GdAlO with minimum deterioration in the charge retention property. © 2010 American Institute of Physics. [doi:10.1063/1.3309693]

Charge-trap-type nonvolatile flash memory is considered to be suitable for further scaling of flash memory devices.¹⁻³ Most of charge-trap-type memory flash memory devices use the TANOS (TaN gate electrode—Al₂O₃ blocking oxide—Si₃N₄ charge trapping layer—SiO₂ tunnel oxide—silicon substrate) structure.⁴ However, the relatively low dielectric constant (~9) of the Al₂O₃ blocking oxide sets a limitation for further scaling of these devices. In order to meet the requirements of both a fast operating speed and good charge retention in further scaled devices, a blocking layer with a higher *k* value without much sacrifice of the conduction band offset is required.⁵ Among high-*k* oxide candidates, gadolinium oxide possesses desirable properties for this type of blocking layer, such as a relatively high dielectric constant (17),⁶ a large band gap (6.4 eV),⁷ and a large conduction band offset (3.1 eV).⁷ It was shown in a previous report that sputtered Gd₂O₃ had the advantages of a faster erase speed and comparable charge retention compared to a Al₂O₃ blocking layer in charge-trap-type flash memory.⁸ Further improvement of the charge retention characteristics was also reported after an addition of aluminum into gadolinium oxide through a cosputtering process.⁹ However, there is no detailed study for the physical properties of gadolinium-aluminum oxide. This paper presents the structural and compositional dependence of gadolinium-aluminum oxide (GdAlO) on the physical and electrical properties of the memory devices with a GdAlO blocking layer.

After a standard gate precleaning process, a 4.5 nm thick tunnel oxide (SiO₂) was thermally grown on a p-type Si substrate and a 6.0 nm thick Si₃N₄ layer was deposited by low-pressure chemical vapor deposition to form the charge-trapping layer. Blocking oxides of Al₂O₃, GdAlO, and Gd₂O₃ were deposited using an atomic layer deposition

(ALD) method using the Eureka 3000 by Jusung Engineering. For the ALD process, trimethyl aluminum and Gd(ⁱPrCp)₃ precursors provided by UP Chemical Co. were used to form Al₂O₃ and Gd₂O₃ films, respectively, with ozone used as an oxidant. The gadolinium percentage in the GdAlO layer was controlled by adjusting the ALD cycles of the Al₂O₃ and Gd₂O₃. For comparison, the thickness of each high-*k* blocking oxide layer was selected so that the equivalent oxide thickness (EOT) of the entire gate stack was similar (~13.5 nm). A 200 nm thick TaN layer was deposited for the metal gate by reactive sputtering. After the patterning of the gate electrode and source/drain implantation, a rapid thermal annealing process was done at 900 °C for 30 s in a N₂ ambient for dopant activation. X-ray photoelectron spectroscopy (XPS) measurements were carried out to measure the atomic concentration, band gap, and band offset. The thickness of each high-*k* blocking oxide was measured by a spectroscopic ellipsometer.

A low leakage current of the blocking oxide is important to improve the erase speed and enhance the erase window by minimizing the electron back-tunneling action from the gate during erase operations. Figure 1 shows the leakage current density of GdAlO films with a various percentages of gadolinium. The 0% Gd and the 100% Gd concentrations in the figure refer to pure aluminum oxide and pure gadolinium oxide, respectively. The leakage current of the GdAlO film was evaluated using whole gate stack (GdAlO/Si₃N₄/SiO₂ tunnel oxide) devices that simulated actual charge-trap devices, as illustrated in the inset of Fig. 1. Because high-*k* dielectric properties such as nucleation and interface reaction depend on the substrate, it would be more useful to compare the properties using the actual device structure which the high-*k* is to be applied for. The Si₃N₄ and SiO₂ thicknesses were fixed at 6 nm and 4.5 nm, respectively. The result shows that the GdAlO devices have much lower leakage current and higher dielectric breakdown voltages compared to the Al₂O₃ device. For easy recognition of the Gd percentage

^{a)}Author to whom correspondence should be addressed. Electronic mail: bjcho@ee.kaist.ac.kr.

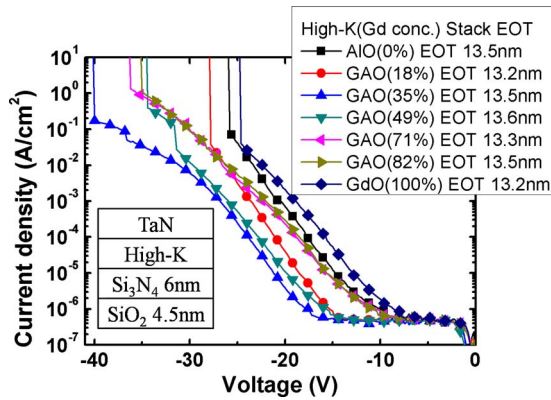


FIG. 1. (Color online) The leakage current density of GdAlO devices with 0%, 18%, 35%, 49%, 71%, 82%, and 100% Gd. The leakage current was evaluated on $\text{Si}_3\text{N}_4(6.0 \text{ nm})/\text{SiO}_2(4.5 \text{ nm})$ (see inset figure). All samples were annealed at 900°C for 30 s as the simulating source/drain annealing step.

dependence on the dielectric properties, the leakage current density at a fixed voltage of -20 V (filled symbols) is plotted as a function of the Gd percentage together with the erase window (open symbols) in Fig. 2(a). The reason for comparing the erase characteristics rather than both program/erase is that the program speed does not change much by changing the blocking oxide layer if the EOT of the gate stack is the same. However, when the blocking oxide is leaky, there will be significant electron back-tunneling from the gate electrode during erase operation, which results in early saturation of the erase state, leading to smaller erase window. Hence, the erase operation is more sensitive to the property of the blocking oxide layer. From the result in Fig. 2(a), it is interesting to note that the leakage current density decreases with the Gd percentage up to 35% and then bounces back for a higher Gd percentage. The erase window also shows the similar trend, as expected. On the other hand, the dielectric constant of the GdAlO film increases steadily with the Gd percentage, as shown in Fig. 2(b). As the final EOT values of the tested GdAlO films are similar, the physical thickness of GdAlO film with a higher Gd percentage is thicker. Despite the increase in the physical thickness, the leakage current increases beyond 35% of Gd in GdAlO.

To investigate the mechanism behind this unusual behavior of the leakage current, x-ray diffraction (XRD) and XPS analyses were performed for GdAlO with different Gd per-

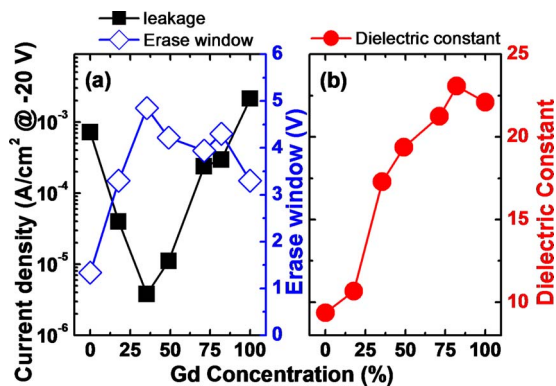


FIG. 2. (Color online) (a) Comparison of the leakage current at -20 V (filled symbols) and erase window (open symbols) and (b) dielectric constant of GdAlO film as a function of the Gd percentage.

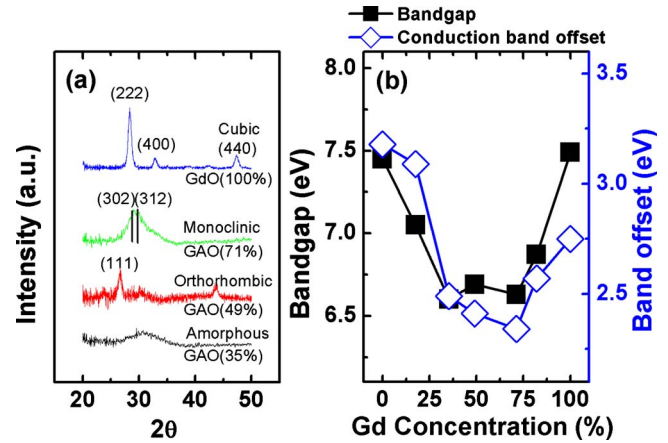


FIG. 3. (Color online) (a) XRD data of GdAlO thin film with 35%, 49%, 71%, and 100% Gd. The crystallized GdAlO film shows many different phases depending on the Gd percentage. (b) The band gap (filled symbols) and the conduction band offset against silicon (open symbols) measured by XPS on GdAlO film directly deposited on silicon. Crystallization of GdAlO results in an increase in the band gap.

centages. Figure 3(a) shows the XRD results of GdAlO thin films with 35%, 49%, 71%, and 100% Gd percentages after annealing at 900°C for 30 s. As expected, a higher Gd percentage in GdAlO resulted in crystallization of the GdAlO film. Surprisingly, however, GdAlO films with 49%, 71%, and 100% Gd showed different phases of orthorhombic, monoclinic, and cubic, respectively. It is also interesting to note that GdAlO with 35% Gd remains amorphous after annealing. This percentage is coincident with the turning point of the leakage current in Fig. 2(a). Therefore, it can be concluded that the increase in the leakage current beyond 35% at Gd is due to the crystallization of the GdAlO film. It is known that the conductivity of the dielectric can be increased by conduction through the grain boundaries of crystallized dielectrics.¹⁰ The band gap and band offset of the GdAlO thin film as a function of the Gd percentage was investigated as well. Using the XPS O 1s energy loss spectra and the valence band spectra,^{11–13} the band gap and valence band offsets were measured and the conduction band offset was determined. These results are shown in Fig. 3(b). It was expected that the band gap of the GdAlO would decrease as the Gd percentage increased considering the reported band gap of Al_2O_3 and Gd_2O_3 films. However, this was true only up to 35% of Gd. Beyond 35% of Gd, no additional decrease in the band gap was observed. The band gap and band offset of GdAlO increase beyond 71% of Gd. The minimum point of the band gap is coincident with the point of the structural change from amorphous to crystalline. The result in Fig. 3 shows that among the crystallized phases, the cubic phase of GdAlO has the highest band gap and band offset. Such band gap widening after crystallization and structural change was also reported in other dielectrics, such as Al_2O_3 .^{13,14}

The manner in which the structural change of GdAlO blocking layer affects the data retention properties in charge-trap-type nonvolatile memory was investigated. The charge retention property was evaluated using a programmed device by monitoring the change in the flat-band voltage (ΔV_{fb}). Here ΔV_{fb} is defined as $V_{\text{fb}}(t) - V_{\text{fb}}(0)$, where $V_{\text{fb}}(t)$ is the flat-band voltage at a certain elapse time during the retention test, and $V_{\text{fb}}(0)$ is the flat-band voltage immediately after program. Three different evaluation criteria were used as fol-

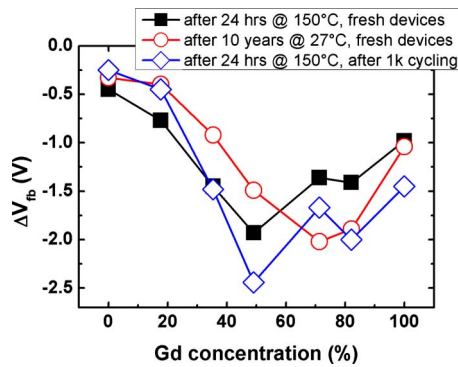


FIG. 4. (Color online) The charge retention property of fresh devices at room temperature (open circle) and 150 °C (filled square) and that of a device cycled for 1000 program/erase at 150 °C (open diamond). Due to the increase of the band gap of the crystallized GdAlO, the charge loss property is improved. However, the crystallized GdAlO is more vulnerable to trap generation during program/erase cycling.

lows: (1) ΔV_{fb} after 24 h at 150 °C, (2) ΔV_{fb} after 11 days at room temperature and then projected to 10 years, and (3) 1000 program and erase cycling followed by measuring ΔV_{fb} after 24 h at 150 °C. The charge loss, represented by ΔV_{fb} is plotted as a function of the gadolinium percentage in Fig. 4. The result shows that at room temperature, $|\Delta V_{fb}|$ increases with the Gd percentage up to 71% and then bounces back and decreases. This indicates that the maximum charge loss occurs at 71% Gd at room temperature. However, at the high temperature of 150 °C, the maximum charge loss occurs at 49% of Gd. The charge loss is then reduced for higher Gd concentrations. It is well known that at a high temperature such as 150 °C, the thermionic emission over the conduction band of the blocking oxide becomes even more important for the charge loss mechanism.¹⁵ The retention data at 150 °C in Fig. 4 resembles very much the band gap and band offset curve in Fig. 3(b). Therefore, the retention data is further evidence of the increase in band gap and band offset for the crystallized GdAlO. When the device is repeatedly programmed and erased, charge traps are formed in the blocking oxide, resulting in degradation of the retention property. The charge loss properties of the GdAlO devices were evaluated after 1000 program/erase (P/E) cycles at 150 °C. This result is shown in Fig. 4 (open diamonds). Compared to P/E cycled and fresh devices, there is no degradation after P/E cycling when the Gd percentage is below 35%. However, noticeable degradation occurs in the devices with Gd percentages of 49% and above, which is the percentage range for the crystallization of GdAlO. This result indicates that crystallized GdAlO is more vulnerable to charge trap generation by electrical stress.

In conclusion, this study showed that the use of GdAlO can significantly reduce the leakage current of the blocking

oxide owing to the physically thicker dielectrics for the same EOT. The reduced leakage current leads to an improvement of the erase window. When the Gd percentage is high, the film is crystallized into many different phases depending on the Gd percentage. The crystallization of the GdAlO film causes a change of the band gap of the GdAlO film, resulting in a change of the retention properties. It was also found that once GdAlO is crystallized, the film becomes more vulnerable to trap generation. Therefore, for the design of flash memory devices, it is necessary to consider the trade-off relationship between the erase window and retention properties which depend on the Gd concentration in GdAlO film.

This work was financially supported by Hynix Semiconductor Inc. The authors would like to thank Jusung Engineering Co. and UP Chemical Co. for the ALD equipment and the precursor supports, respectively.

- ¹K. Kim and J. Choi, *Proceedings of the IEEE Nonvolatile Semiconductor Memory Workshop 2006* (IEEE, Monterey, CA, 2006), p. 9.
- ²Y. Park, J. Choi, C. Kang, C. Lee, Y. Shin, B. Choi, J. Kim, S. Jeon, J. Sel, J. Park, K. Choi, T. Yoo, J. Sim, and K. Kim, *Tech. Dig. - Int. Electron Devices Meet.* **2006**, 346900.
- ³C. H. Lee, K. I. Choi, M. K. Cho, Y. H. Song, K. C. Park, and K. Kim, *Tech. Dig. - Int. Electron Devices Meet.* **2003**, 613 (2003).
- ⁴C. H. Lee, C. Kang, J. Sim, J. S. Lee, J. Kim, Y. Shin, K. T. Park, S. Jeon, J. Sel, Y. Jeong, B. Choi, V. Kim, W. Jung, C. I. Hyun, J. Choi, and K. Kim, *Proceedings of the IEEE Nonvolatile Semiconductor Memory Workshop 2006* (IEEE, Monterey, CA, 2006), p. 54.
- ⁵J. A. Kittl, K. Opsomer, M. Popovici, N. Menou, B. Kaczer, X. P. Wanga, C. Adelman, M. A. Pawlak, K. Tomida, A. Rothschild, B. Govoreanu, R. Degraeve, M. Schaekers, M. Zahid, A. Delabie, J. Meerschaert, W. Polspoel, S. Clima, G. Pourtois, W. Knaepen, C. Detavernier, V. V. Afanas'ev, T. Blomberg, D. Pierreux, J. Swerts, P. Fischer, J. W. Maes, D. Manger, W. Vandervorst, T. Conard, A. Franquet, P. Favia, H. Bender, B. Brijis, S. Van Elshocht, M. Jurczak, J. Van Houdt, and D. J. Wouters, *Microelectron. Eng.* **86**, 1789 (2009).
- ⁶W. H. Chang, C. H. Lee, P. Chang, Y. C. Chang, Y. J. Lee, J. Kwo, C. C. Tsai, J. M. Hong, C.-H. Hsu, and M. Hong, *J. Cryst. Growth* **311**, 2183 (2009).
- ⁷T. Hattori, T. Yoshida, T. Shiraishi, K. Takahashi, H. Nohira, S. Joumori, K. Nakajima, M. Suzuki, K. Kimura, I. Kashiwagi, C. Ohshima, S. Ohmi, and H. Iwai, *Microelectron. Eng.* **72**, 283 (2004).
- ⁸J. Pu, S. J. Kim, Y. S. Kim, and B. J. Cho, *Electrochem. Solid-State Lett.* **11**, H252 (2008).
- ⁹J. Pu, D. S. H. Chan, S. J. Kim, and B. J. Cho, *IEEE Trans. Electron Devices* **56**, 2739 (2009).
- ¹⁰O. Bierwagen, L. Geelhaar, X. Gay, M. Piešiš, H. Riechert, B. Jobst, and A. Rucki, *Appl. Phys. Lett.* **90**, 232901 (2007).
- ¹¹S. Miyazaki, H. Nishimura, M. Fukuda, L. Ley, and J. Ristein, *Appl. Surf. Sci.* **113-114**, 585 (1997).
- ¹²H. Y. Yu, M. F. Li, B. J. Cho, C. C. Yeo, M. S. Joo, D.-L. Kwong, J. S. Pan, C. H. Ang, J. Z. Zheng, and S. Ramanathan, *Appl. Phys. Lett.* **81**, 376 (2002).
- ¹³S. Miyazaki, *J. Vac. Sci. Technol. B* **19**, 2212 (2001).
- ¹⁴V. V. Afanas'ev and A. Stesmans, *J. Appl. Phys.* **102**, 081301 (2007).
- ¹⁵A. Arreghini, N. Akil, F. Driussi, D. Esseni, L. Selmi, and M. J. van Duuren, *Solid-State Electron.* **52**, 1460 (2008).